Machine Vision and Applications (2006) 16(6): 374–383
DOI 10.1007/s00138-005-0009-8

ORIGINAL PAPER

J. Jay Liu · John F. MacGregor

Estimation and monitoring of product aesthetics: application to manufacturing of "engineered stone" countertops

Received: 5 October 2004 / Accepted: 30 September 2005 / Published online: 6 January 2006

Abstract A new machine vision approach for *quantitatively* estimating and monitoring the appearance and aesthetics of manufactured products is presented. The approach is composed of three steps: (1) wavelet-based textural feature extraction from product images, (2) estimation of measures of the product appearance through subspace projection of the textural features, and (3) monitoring of the appearance in the latent variable subspace of the textural features. The methodology is specifically designed to treat the *stochastic* nature of the visual appearance of many manufactured products. This nondeterministic aspect of product appearance has been an obstacle for the success of machine vision in many industries. The emphasis of this approach is on the consistent and quantitative estimation of continuous variations in visual appearance rather than on classification into discrete classes. This allows for the on-line monitoring and the eventual feedback control of product appearance. This approach is successfully applied to the estimation and monitoring of the aesthetic quality of manufactured stone countertops.

Keywords Engineered stone countertops · Machine vision · Monitoring · Visual appearance · Wavelet texture analysis · Principal component analysis

1 Introduction

Machine vision has been studied for about 40 years. But the research in the last 15 years has shown rapid progress because of the advances in computing and imaging technologies and its subject now includes countless topics and applications. Automatic assembly and inspection in the manufacturing industries, verification of signatures, checking of fingerprints and recognizing faces and iris for personal identification, and analysis of remotely sensed images in geoscience are just a fraction of the entire list [1, 2]. Machine vision can be defined as "interpretation of an image of an object or scene through the use of optical noncontact sensing mechanisms for the purpose of obtaining information and/or controlling machines or processes" [2]. It is clear from this definition that the main purpose of machine vision is "to allow a computer to understand aspects of its environment using information provided by visual sensors" [2] and thus it requires a combination of image processing to enhance the image quality and pattern recognition and image analysis to recognize features present in the image [3].

Automatic inspection and assembly is one application area in which machine vision has been very successful and it is still growing substantially. The driving force for this growth is the necessity of improvements in quality, safety, and cost saving. However, according to Marshall and Martin [2], most successful techniques and their applications in machine vision research have been confined to a specific type of environment where certain assumptions can be made about the scene. In typical manufacturing industries such as printed circuit boards (PCBs) fabrication, for example, an image contains a scene of objects with *pre-determined* shape, structure, orientation, and so on. In other words, scenes in images from such industries are *deterministic*. The primary goal of the inspection in such manufacturing industries is to check whether there are missing objects in prespecified regions in the image or whether objects in the image are in desired orientations or of desired size. The necessary analysis as well as image processing is mainly done directly on the image itself.

On the other hand, in the process industries there is a different class of problems where the major concern is some ill-defined visual appearance of products or processes. Examples include, but not limited to, the color and appearance of mineral flotation froth [4], visible patterns such as stripes and swirls on the surfaces of injection-molded plastic panels [5], or the surface quality of rolled steel sheets [6]. In such

J. J. Liu (✉) · J. F. MacGregor
Department of Chemical Engineering, McMaster University,
1280 Main Street West, Hamilton, Ontario, L8S 4L7, Canada
E-mail: macgreg@mcmaster.ca

Present Address. Samsung Electronics, Asan, Chungcheongnam-Do, Korea

cases, simple assumptions about the scene can no longer be made because of the *stochastic* nature of the visual appearance of the products/processes. For this reason, machine vision has rarely been applied to those problems and has had little success when it has. In the example of injection-molded plastic panels, the panels can contain visible patterns such as stripes, swirls, and ripples with *varying* characteristics in their shapes, directions, and intensities [5]. There exists *no* distinct class of patterns in the panels since different visible patterns can merge together to form more complicated patterns. Depending on the number and the types of basic patterns merged and their varying characteristics, there can be *infinite* number of patterns in the panels. Because of this stochastic nature, the state or the quality of the appearance of these processes or products is almost always judged by trained human operators and any control actions are left to their decisions at the present time. For this reason, *inconsistency* in human judgment still remains a critical issue in the process industries.

The contribution of this paper is to illustrate a new machine vision approach for the manufacturing industries that is capable of assessing and monitoring the visual quality of manufactured products. In this approach, machine vision will include new application areas and new tasks that have seldom been tried in contemporary machine vision research. New application areas include all manufacturing industries where the stochastic visual appearance of products or processes is important. New tasks include estimation, monitoring, and control of the visual quality of the process or the product. Visual quality studied in this paper means textural appearance of processes and products. The rest of this paper is organized as follows: In Sect. 2, a new machine vision approach is presented by combining methods such as wavelet texture analysis, latent variables methods for the quantitative estimation of visual quality from textural information, and multivariate statistical process control (MSPC) of visual quality. The illustration of this new approach is then given via an industrial application to the visual appearance of manufactured countertops in Sect. 3. Summary and conclusion are given in Sect. 4.

2 Machine vision for the process industries

2.1 Extracting textural information from the product images

The appearance or aesthetics of a product usually depend on a combination of color and textural properties of a product surface. In the manufactured stone countertops in Sect. 3 of this paper, the appearance of countertops is essentially grayscale and thus it is related *only* to textural properties. Therefore, we will focus on the extraction of textural properties via two-dimensional wavelet transforms. However, there are many works on the extraction of spectral information from color images [7, 8] and some recent work on combining both spectral and textural analysis [4, 9], which can be easily integrated into the approach and be used for the *colored* engineered stone countertops manufacturing.

2.1.1 Wavelet transform

The continuous wavelet transform (CWT) of a signal $f(s)$ is defined by the convolution integral

$$\mathrm{CWT}\,(a,\tau) = \frac{1}{\sqrt{a}} \int f(s)\psi\left(\frac{\tau - s}{a}\right) \mathrm{d}s \tag{1}$$

where a and τ are continuous scale and shift parameters, respectively. Equation (1) can be interpreted as the *correlation* of the input signal with a time-reversed and rescaled (by a factor a) $\psi(s)$. The magnitude of the coefficient is maximized when the frequency of the signal matches that of the corresponding dilated wavelet.

The discrete wavelet transform (DWT) computes the CWT at dyadic scale $a = 2^j$ and $\tau = 2^j k$ ($j \in Z^+, k \in Z$). The computational complexity is O(N) using either Mallat's algorithm or the "Algorithme à trous" [10, 11]. The mother wavelet $\psi(s)$ is related to the scaling function $\phi(s)$ with some suitable sequence $h[k]$ [10–13];

$$\psi(s) = \sqrt{2}\sum_k h_1[k]\phi(2s - k), \tag{2}$$

where $\phi(s) = \sqrt{2}\sum_k h_0[k]\phi(2s-k)$ and $h_1[k] = (-1)^k h_0[1-k]$. Using the following relations, the DWT at decomposition level j can be performed *without* requiring the explicit forms of $\psi(s)$ and $\phi(s)$;

$$\phi_{j,l}[k] = 2^{j/2} h_0^{(j)}[k - 2^j l], \tag{3}$$

$$\psi_{j,l}[k] = 2^{j/2} h_1^{(j)}[k - 2^j l]. \tag{4}$$

where $h_m^{(j+1)}[k] = [h_m]_{\uparrow 2^j} \times h_m^{(j)}[k]$ and $h_m^{(0)}[k] = h_m[k]$ ($m = 0, 1$), $[\cdot]_{\uparrow 2^j}$ denotes up-sampling by a factor of 2^j, j and l are the scale and translation indices, respectively.

The DWT coefficients of a signal $f(s)$ are now computed as

$$a_{(J)}[l] = \left\langle f[k], \phi_{J,l}[k] \right\rangle \quad \text{and} \quad d_{(j)}[l] = \left\langle f[k], \psi_{j,l}[k] \right\rangle, \tag{5}$$

where the $a_{(J)}[l]$'s are expansion coefficients of the scaling function or approximation coefficients and the $d_{(j)}[l]$'s ($j = 1, 2, \ldots, J$) are the wavelet coefficients or detail coefficients. Among several solutions for achieving a two-dimensional (2D) DWT, a separable solution is very easy to design and implement compared to nonseparable solutions [13]. It gives rectangular divisions of frequency spectrum and strongly oriented coefficients (often called *subimages* because the wavelet coefficients for 2D signals are also 2D) in the horizontal, vertical, and diagonal directions. This separable solution (Mallat's algorithm for the 2D DWT) is illustrated in Fig. 1. However, when texture is isotropic, even

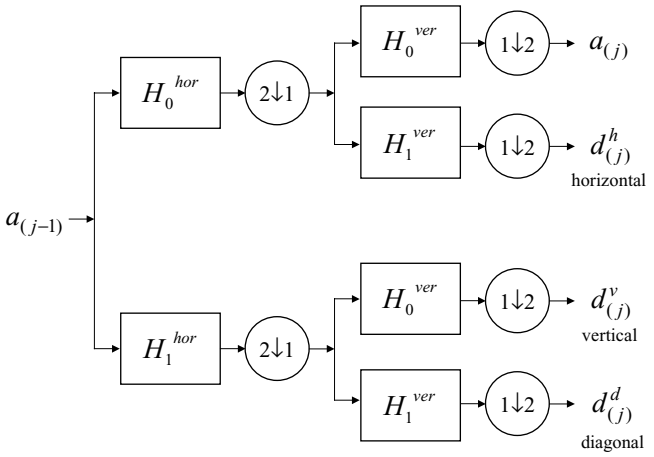

Fig. 1 A separable solution for 2D DWT. A separable 2D filter bank at the jth decomposition stage. It consists of horizontal and vertical filtering of 2D signals using low-pass and high-pass 1D wavelet filters H_0 and H_1. Separable horizontal ($2\downarrow1$) and vertical ($1\downarrow2$) down-sampling by 2 gives a separable sampling lattice

small rotation can have a drastic change in the results obtained using the separable 2D DWT. This problem can be avoided by using the nonseparable 2D DWT or by using a simple transformation that is used in this paper (see next section).

2.1.2 Wavelet texture analysis

Among other texture analysis methods, *wavelet texture analysis* (WTA), a 2D DWT-based method, seems best not only because it has shown better performance than other methods in many cases [6, 14] but also there is strong psychophysical evidence that the human visual system does multi-channel, space–frequency analysis [15]. WTA was successfully applied to characterization of steel surface, estimation of visual appearance of injection-molded plastic panels, and flotation froth monitoring in previous studies [4–6].

A basic assumption for WTA is that a texture has its unique distribution (i.e., energy or entropy distribution) in the 3D scale–space consisting of spatial axes and an additional scale axis. Therefore, if the scale axis of the scale–space of a textured image is discretized appropriately, different textures will have different features at the discretized scales. Many works regarding wavelet-based feature detection/extraction are based on this assumption. If a wavelet subimage (i.e., $a_{(J)}$ and $d^k_{(j)}$ where $j = 1, 2, \ldots, J$ and $k = h, v, d$ for a separable 2D DWT. See also Fig. 1) is treated as a matrix, then the power or energy of the subimage can be defined using the Frobenius norm, $||\cdot||_{\mathrm{F}}$. For example, the energy of the approximation subimage $a_{(J)}$ is given as

$$E_{a_{(J)}} = \left\|a_{(J)}\right\|_{\mathrm{F}}^2. \tag{6}$$

Often this is divided by the number of pixels, yielding averaged power or *normalized energy*. A feature vector composed of energies of all subimages is often called *wavelet energy signature*, one of the most popular wavelet textural features. Since the mean values of detail subimages are equal to zero, the normalized energy of each subimage is equal to variance of a corresponding channel (after mean-centering for the approximation subimage). Therefore, the wavelet energy signature also represents *contrast information* of subimages.

The idea of WTA based on the 2D DWT can also be extended to 2D wavelet packets (WP) with an arbitrary tree structure [16–18]. When an image is decomposed down to the Jth level, the size of a feature vector for an image (when including an approximation subimage) is $3J+1$ for the 2D DWT and 4^J for the 2D full-tree WP, respectively.

2.2 Quantitative estimation of visual quality in latent variable spaces

In addition to the selective feature extraction of the human visual system, the human brain can reduce the dimension of the extracted information and analyze it. For example, operators evaluate the quality of steel surfaces as good, medium, and bad [6], or evaluate the aesthetic quality of manufactured countertops as on-specification and off-specification by looking at an image or a scene that can be easily of several megabytes and hundreds of thousands of pixels. Therefore, an additional step is required to further simplify and condense the information of the extracted feature vector into a smaller number of features that represent all the important and consistent information in the feature vector in a more efficient manner.

For this reason, further dimensional reduction is desirable after extracting wavelet textural features from images and it can be done using a method such as Principal Component Analysis (PCA) [19–21]. Fisher's Discriminant Analysis (FDA) [22] can be used when class labels are available, and Independent Component Analysis (ICA) [23] and Projection Pursuit (PP) [24] can also be used on the PCA scores (called *pre-whitening* by PCA). This additional compression step is *necessary* for handling the stochastic nature of the visual appearance and is a *crucial* element in the new machine vision approach proposed in this paper. All these linear projection methods find an operator that can map high-dimensional feature space to a low-dimensional latent variable subspace and they are perfect candidates in estimating visual quality. Let $\boldsymbol{x}$ be a $(K \times 1)$ feature vector after 2D DWT of an image and followed by a nonlinear transform (e.g., $||\cdot||_{\mathrm{F}}$) and $\boldsymbol{t}$ be a $(A \times 1)$ latent vector after dimensionality reduction. Then the following equality holds via a $(A \times K)$ mapping matrix $\boldsymbol{W}$:

$$\boldsymbol{t} = \boldsymbol{W}\boldsymbol{x} \tag{7}$$

The matrix $\boldsymbol{W}$ is called a *loading* matrix in PCA and a separating or unmixing matrix in ICA.

In any linear projection method, the rows of the mapping matrix represent *contributions* of features $\boldsymbol{x}$ to each of

the latent variables in $\boldsymbol{t}$ because each latent variable is simply a linear combination of features with elements in each row of the mapping matrix as coefficients. Therefore if features have certain psychophysical meanings then we can also give a psychophysical meaning to each latent variable. This is crucial when we *numerically* estimate visual quality and this is the one reason why we choose projection methods for feature reduction. Another crucial reason is that the visual quality of products and/or processes of interest is *not* a discrete or disjoint quality as in typical classification tasks, rather it is a *continuous* quality [4–6]; For example, quality of steel surface *gradually* deteriorates from good to medium and from medium to bad, and the state of a mineral flotation process *gradually* changes depending on the amount of chemical reagents added, the mineral content of the ore, and the state of previous flotation cells. Therefore using projection methods and working with *continuous latent variables* to provide a continuous quantitative estimate of appearance is more suitable in this circumstance than using classification methods and working with discrete class labels. This quantitative estimation then allows for on-line monitoring and feedback control of the visual appearance of products.

2.3 Monitoring of visual quality in latent variable spaces

In statistical process control (SPC), a set of data $\boldsymbol{X}$ is obtained when a process is *in control* (i.e., under normal operation). In general, this set consists of observations, i.e. row vectors of process variables and/or product variables but in our case, it consists of textural feature vectors extracted from product images. Therefore, each row of $\boldsymbol{X}$ corresponds to $\boldsymbol{x}^{\mathrm{T}}$, the transpose of a textural feature vector $\boldsymbol{x}$. PCA then allows for the representation of the $(m \times K)$ feature matrix $\boldsymbol{X}$ in terms of a reduced $(m \times A)$ dimension matrix of latent variables $(\boldsymbol{T})$ as:

$$\boldsymbol{X} = \boldsymbol{T}\boldsymbol{W} + E \tag{8}$$

where m is the number of observation (i.e., the number of images in this paper), $\boldsymbol{E}$ is a residual matrix $(m \times K)$, and the rows of $\boldsymbol{T}$ $(m \times A)$ consists of $\boldsymbol{t}^{\mathrm{T}}$, the transpose of a latent vector. A latent vector, $\boldsymbol{t}$ $(A \times 1)$ is the projected location of an observation, $\boldsymbol{x}$ $(K \times 1)$ in the latent variable space where $K \gg A$. The distance of $\boldsymbol{x}$ from the latent variables space, often called squared prediction error (SPE), provides a measure of how close this observation is to the A-dimensional latent variable space [25, 26]:

$$\begin{aligned} \mathrm{SPE}_{\boldsymbol{x}} &= \boldsymbol{e}^{\mathrm{T}}\boldsymbol{e} \\ &= \|\boldsymbol{x} - \hat{\boldsymbol{x}}\|^2 \\ &= \boldsymbol{x}^{\mathrm{T}}(\boldsymbol{I} - \boldsymbol{W}^{\mathrm{T}}\boldsymbol{W})\boldsymbol{x} \end{aligned} \tag{9}$$

where $\boldsymbol{I}$ is the identity matrix. This is sometimes referred to as the Q statistics or distance to the model (DModX).

From the data $\boldsymbol{X}$ collected under the normal operation, the projection matrix, $\boldsymbol{W}$ that provides the low dimensional model for the normal operating region is determined. Whenever a new observation, $\boldsymbol{x}_{\mathrm{new}}$ is available, the corresponding latent variables $\boldsymbol{t}_{\mathbf{new}}$ $(=\boldsymbol{W}\boldsymbol{x}_{\mathrm{new}})$ and $\mathrm{SPE}_{\boldsymbol{x}\mathbf{new}}$ $(=\boldsymbol{x}_{\mathrm{new}}^{\mathrm{T}}(\boldsymbol{I} - \boldsymbol{W}^{\mathrm{T}}\boldsymbol{W})\boldsymbol{x}_{\mathrm{new}})$ can be calculated and checked against normal operation using $\boldsymbol{W}$. In monitoring using PCA for example, Hotelling's T^2 statistic is used for monitoring scores [27]:

$$\boldsymbol{T}^2 = \boldsymbol{t}_{\mathrm{new}}^{\mathrm{T}}\Lambda_A^{-1}\boldsymbol{t}_{\mathrm{new}} \tag{10}$$

where Λ_A^{-1} is a diagonal matrix of the inverse of A eigenvalues of a sample covariance matrix of $\boldsymbol{X}$ corresponding to the principal components retained. For a given significance level α, the upper control limit is given as [27]

$$T^2_{\mathrm{UCL}} = \frac{A(m-1)}{m-A}F_\alpha(A, m-A) \tag{11}$$

where $F_\alpha(A, m-A)$ is the upper $100\alpha\%$ critical point of the F distribution with $(A, m-A)$ degrees of freedom. For the SPE, the upper control limit can be computed for a given significance level α as in [26, 27].

It is well known in the statistical process control literature [25–27] that the SPE and the Hotelling T^2 are complementary and not alternative statistics. Hotelling T^2 statistic is a measure of the distance from the origin (center of the region of normal operation) of the scores obtained from of the projection of a feature vector x onto the PCA model space. It measures the magnitude of the current process operation from normal behavior in the space of the PCA model. On the other hand, the SPE statistic is a model residual for the feature vector x, and it is a measure of the orthogonal distance of the new feature vector from the model plane. The distance within the model plane (T^2) and the residual (SPE) orthogonal to the model plane must be below their control limits for the product to be deemed in a state of control. For on-line multivariate statistical process control (MSPC), abnormal product appearance would then be indicated by either one of the SPE or Hotelling's T^2 statistics falling outside their control limits [25, 26]. The monitoring using ICA can be done in a similar context. Monitoring statistics regarding ICA (such as I^2) can be found in [28].

3 Application to the characterization and SPC of manufactured stone countertops

3.1 Description of data

The image data set consists of sixteen 24-bit 1024×1024 grayscale images of manufactured countertop slabs made of natural quartz and plastic resin (often called engineered stone). For imaging, 16 batch operations with different recipes and different operating conditions were selected and one countertop slab was collected from each batch yielding 16 slab samples with variations in countertop patterns. Four samples of countertop slabs with qualitative evaluations on patterns by operators/engineers are shown in Fig. 2. It is not very difficult for an untrained person to observe some difference in an appearance or aesthetic quality of the four countertops (at least the extreme qualities such as slab numbers

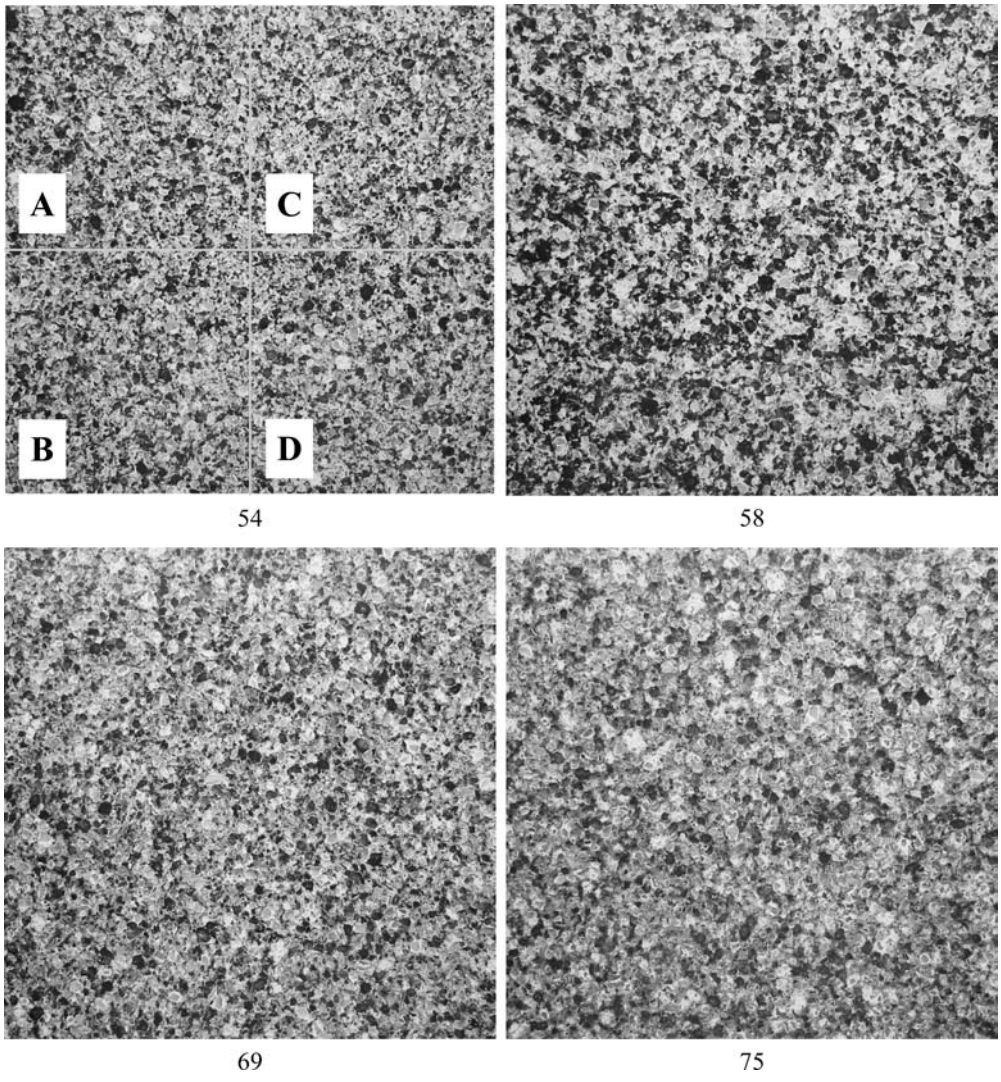

Fig. 2 Four sample images of countertop slabs. Experts' evaluations are as follows: slab number 54, "too much area with fine scale structure"; 58, "high contrast"; 69, "on aim pattern"; and 75, "coarse pattern." In Sect. 3.2, all images are subdivided into four smaller images as shown in slab 54

58 and 75), or to agree with the evaluations on the aesthetic quality given by the industrial personnel. However, apart from the consistency issue in human judgment, it is *very* difficult to characterize the aesthetic quality of a countertop in terms of several specific criteria. In this application even the experts did not have such criteria yet and therefore, the qualitative evaluations on aesthetic quality of countertops were not available for all 16 slabs. Furthermore, there is *no* distinct set of classes one can define and classify since the texture of countertops is determined by a complex combination of different recipes of plastic resin and quartz, and different process operating conditions. It is impossible to produce countertops that are *pixel-by-pixel* identical. From the viewpoint of plant operation, this hard-to-define and stochastic visual pattern (i.e. the aesthetic quality of a manufactured countertop) is a target to be controlled or monitored. Therefore, the objective of this research was to develop a quantitative measure of differences in stochastic appearance to enable the industrial personnel to judge differences, to set targets, and to perform on-line monitoring of the appearance or aesthetic quality of the countertops.

3.2 Estimation of visual quality

Each original countertop image was subdivided into four nonoverlapping (512 × 512) smaller images (see slab number 54 in Fig. 2). These subdivided images are considered as within-batch products (i.e., products from the same batch) in this study. Therefore, a new image set has 64 images, with four images from the same batch operation. A total of 48 images (i.e., three images per batch) are selected for training and 16 images (i.e., one image per batch) for testing. For feature extraction, four-level 2D DWT was applied to all 64 images using order-one Coiflet filters and an energy signature (13 × 1) was calculated from 13 wavelet subimages

(a_4 and $d^k_{(j)}$; $k \in h, v, d$ and $j \in 1, 2, 3, 4$) for each of 64 images (each approximation subimage was mean-centered before calculating energy). These choices (the number of decomposition levels and the wavelet filter used) were made by trial and error but following some guidelines [26, 29]. For example, the number of decomposition stages was determined according to our experience such that the size of the smallest subimage should be greater than 10×10 and this criterion is conformable to that of Chang and Kuo [16].

A preliminary analysis by Principal Component Analysis (PCA) of the autoscaled (i.e., mean-centered and unit-variance scaled) (48×13) matrix composed of energy signatures of the training images provided loading plots showing a natural clustering of the horizontal (h) and vertical (v) energies of the wavelet subimages in each decomposition level. This is because, when texture is isotropic, horizontal, and vertical wavelet subimages should be identical to each other. Therefore, an average energy (will be denoted as hv later in this section) was calculated from the energies of horizontal and vertical subimages of each decomposition level and used in the subsequent analysis. Each image is then represented by a (9×1) energy signature.

PCA was applied to the pruned (48×9) training data (i.e., energy signatures of 48 training images) after mean-centering using the average energy signature of good batch countertops and unit-variance scaling. Three statistically significant principal components were found on the basis of the Bootstrap risk estimate [30]. R^2 (the fraction of variance of feature vectors explained by the PCA model) and Q^2 (the fraction of variance predicted for images not used in the PCA model) are summarized in Table 1. Two score plots, the corresponding SPE plot (with both training and test images), and three loading plots are shown in Figs. 3–5 respectively. As seen from Table 1, and the score plots and the SPE plot, the variability of countertop slabs in terms of energy signatures is well modeled by the PCA model. As expected, within-batch variations (local variations in the original slabs) are smaller than between-batch variations in the score plots. This also reveals that the aesthetic quality of countertops can be represented by values of the three principal components because visually similar images have score values that lie close to each other and visually different images have score values that lie far apart. Hence, the latent variables of PCA provide a consistent and quantifiable measure of stochastic appearance of countertops.

As in previous studies [4, 5], a careful observation of score plots and loading plots can provide some interpretation of the PCA latent variable space. Although an energy signature of an image provides multiresolution contrast

Table 1 Summary of PCA results

Dimension of latent space	R^2	Q^2
1	0.685	0.592
2	0.918	0.834
3	0.980	0.945

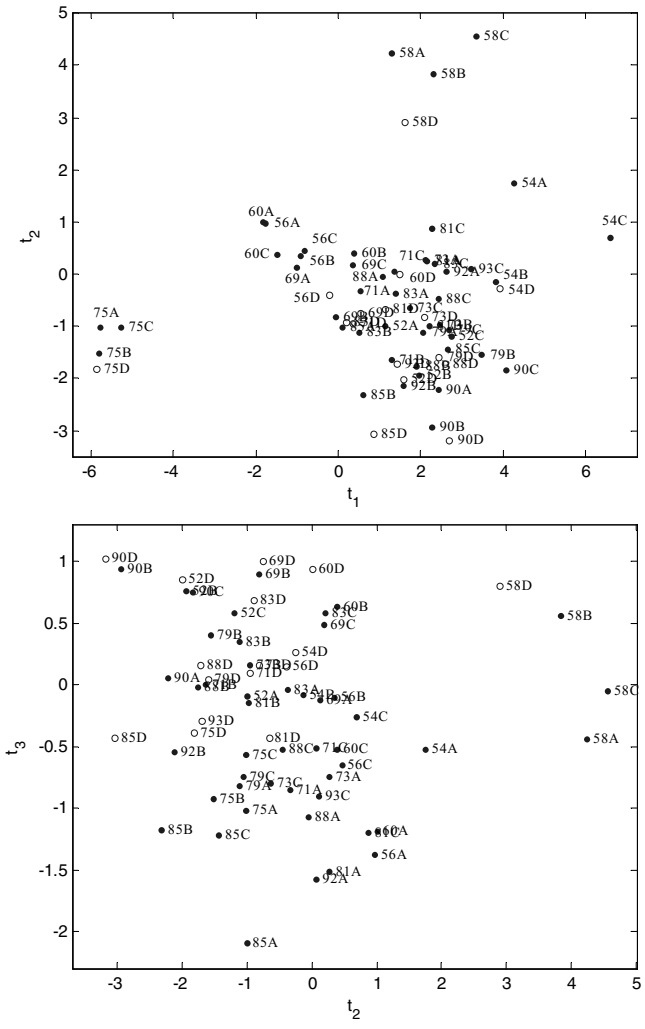

Fig. 3 t_1–t_2 and t_2–t_3 score plots (●: training data, ○: test data)

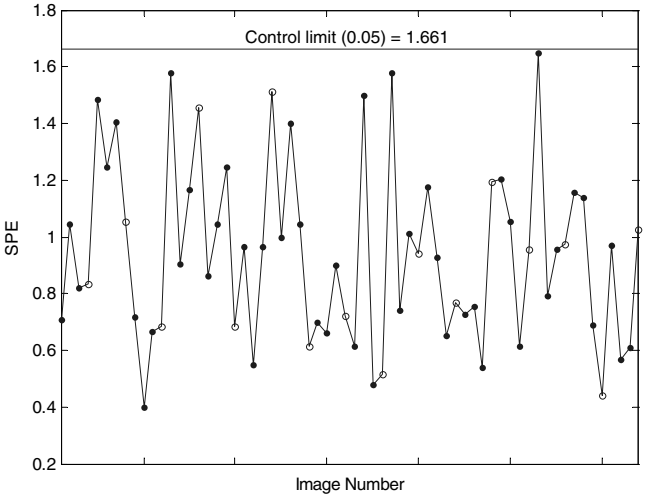

Fig. 4 An SPE (Squared Prediction Error) plot (●: training image data, ○: test image data)

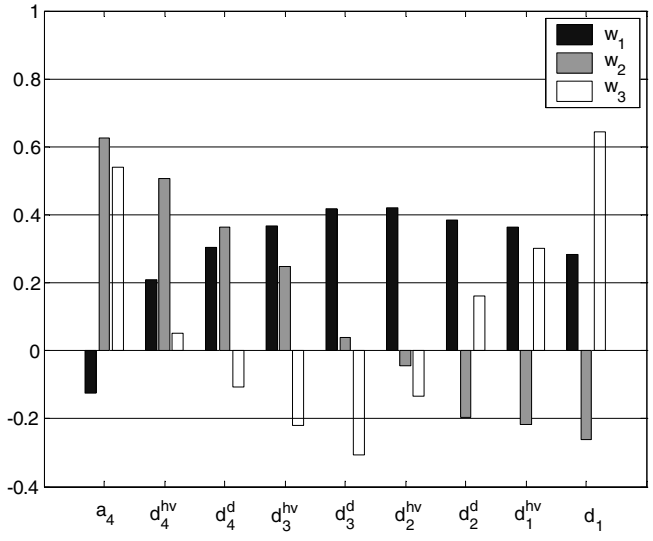

Fig. 5 A w_1, w_2, w_3 loadings plot

information, it may not be directly related to the aesthetic quality of the countertops. However, if a PCA model captures most of the variability of the aesthetic quality in wavelet feature space, then dominant variations in aesthetic quality will be represented by a few principal components that are a linear combination of energies of wavelet subimages. Since the PCA latent variables (t_1, t_2, ...) are linear combinations of these subimage energies, images with almost identical subimage energies will result in PCA score values being very close to one another as seen in Fig. 3. From the w_1 loading plot in Fig. 5, low frequency components in the aesthetic quality represented by the energy of a_4 are dominant in images in the negative t_1 direction and the intermediate and high frequency components (energies of all detail subimages) are dominant in images in the positive t_1 direction. Comparing two slabs (slab numbers 54 and 75 in Fig. 2) at opposite ends of the t_1 axis and the corresponding qualitative evaluations given by the industrial personnel

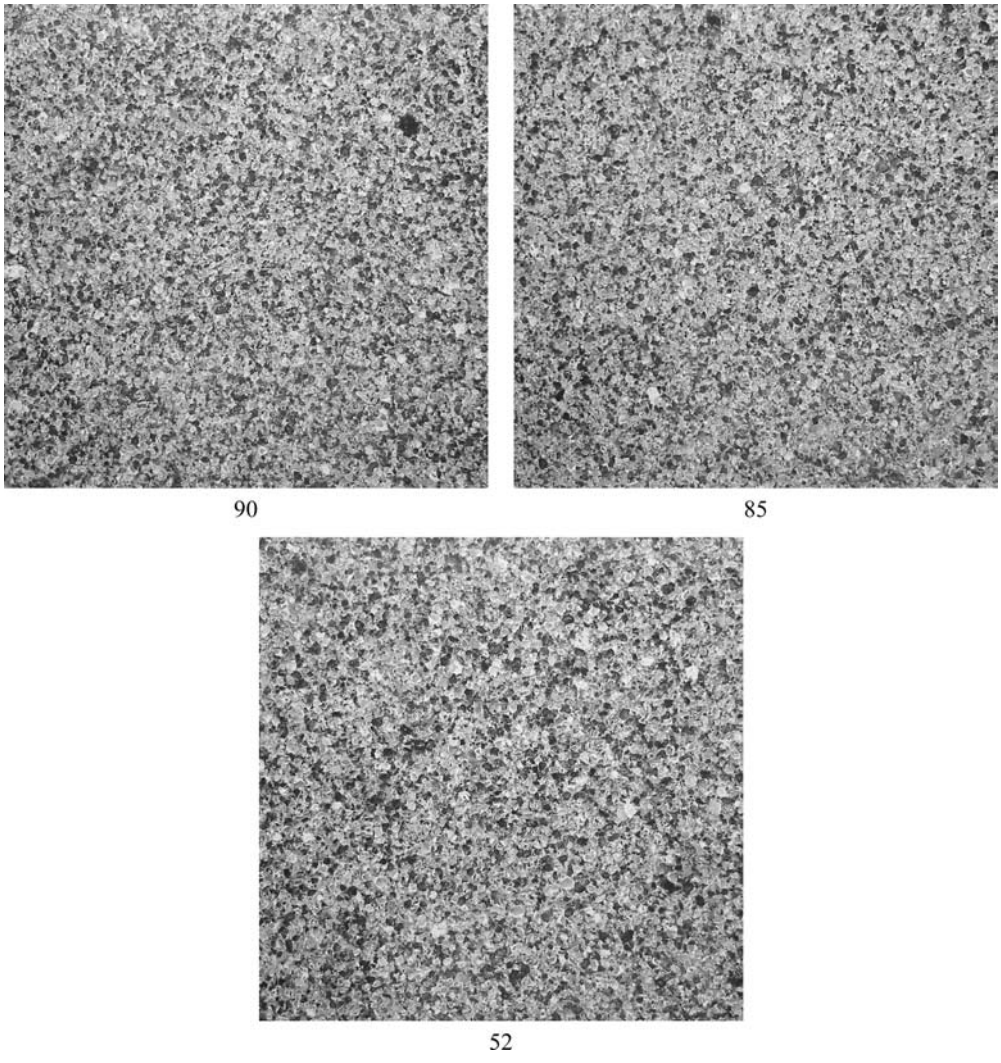

Fig. 6 Slab numbers 90, 85, and 52

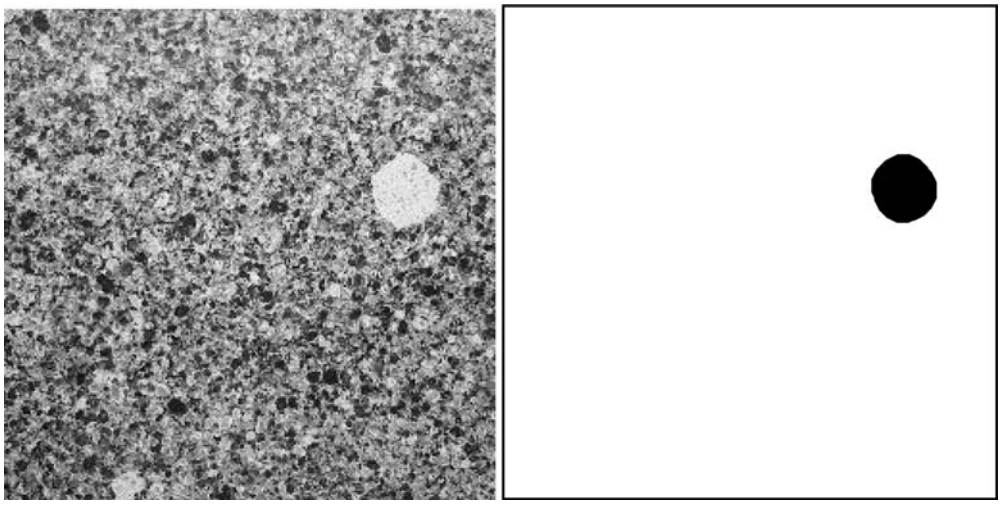

Fig. 7 A "blotch" in slab number 60 (*left*) and a detection result in black (*right*)

(slab number 54: "too much area with fine scale structure"; slab number 75: "coarse pattern") reveal that the first principal component captures some form of *fineness* information in the aesthetic quality of the countertops.

On the other hand, the t_2 direction appears to represent a contrast between low and high frequency energies (see w_2 loading). Slabs in the positive t_2 direction have dominant low to mid frequency components (a_4, d_4^{hv}, d_4^d, and d_3^{hv}) while slabs in the negative t_2 direction have dominant mid to high frequency components (d_2^d, d_1^{hv}, and d_1^d) seen from the w_2 loading plot. It is easy to note that slab number 90 in Fig. 6, which is in the negative t_2 direction in Fig. 3, has low contrast compared to slab number 58 in Fig. 2, which is in the positive t_2 direction and evaluated as "high contrast." These reveal that the second principal component captures some form of *contrast* information in the aesthetic quality of the countertops. Although the w_3 loading plot shows an interesting pattern (positive loadings at both low and high frequencies and negative loadings at intermediate frequencies), interpretation of the psychophysical meaning of the statistically significant third component t_3 is not very clear in the images. This is probably because the most visually dominant characteristics of aesthetic quality are already captured by the first two principal components and the effects captured by t_3 are not easily seen in the raw images. For example, slab numbers 52 and 69 lie in the positive t_3 direction (Fig. 3) and 85 lies in the negative t_3 direction while their t_1 and t_2 score values are almost the same. Because there is some visual distinction between these slabs (52, 69, and 85), the third principal component, t_3 is clearly capturing an aesthetic feature but it is difficult to pinpoint. The only noticeable visual difference seems to be that quartz pieces in slabs 52 and 69 have clearer edges than those in slab 85 in Figs. 2 and 6. Positive contributions of high frequency detail subimages (d_2^d, d_1^{hv}, and d_1^d) in t_3 (see the w_3 plot in Fig. 5) can explain this visual difference.

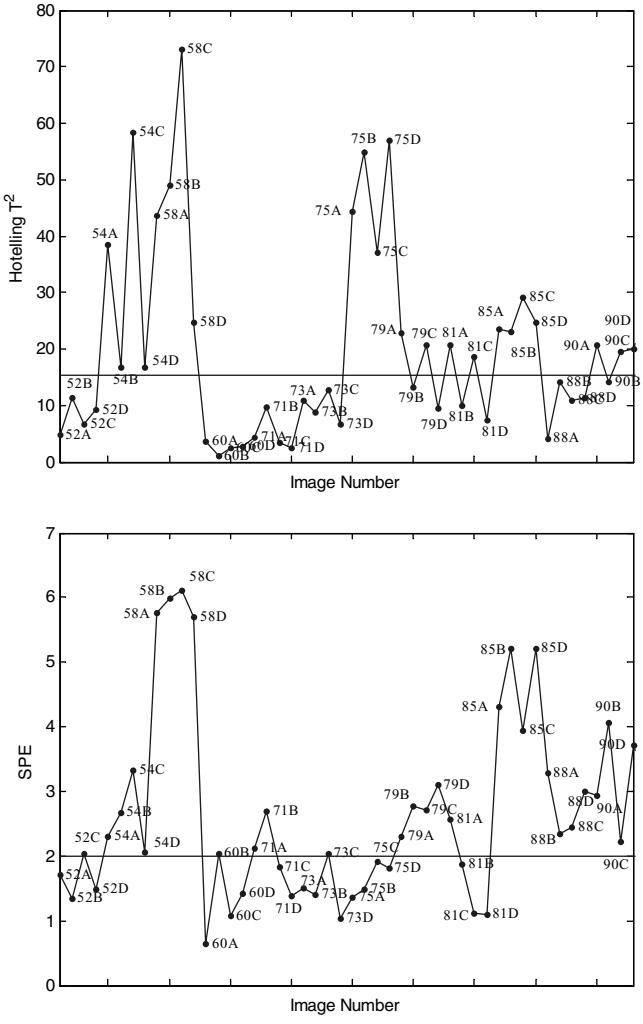

Fig. 8 Hotelling T^2 and SPE charts for detecting off-specification countertops. Control limits ($\alpha = 0.05$) were calculated using 16 countertops from good batches

3.3 Monitoring of aesthetic quality

Before monitoring aesthetic quality, detecting and locating various gross defects is desirable. One type of defect that countertop slabs occasionally have is the "blotch" as shown in Fig. 7. This type of defects can be easily detected and located using morphological operations, dilation and erosion [31]. Using a disk-shaped structuring element with appropriate size, one can detect blotches as shown in the figure, and any countertops containing this defect can be isolated.

After blotch detection, one can use the Hotelling T^2 chart and SPE plot discussed earlier for aesthetic quality monitoring. To detect whether a countertop has off-specification aesthetic quality, a new PCA model was developed using 16 good batch countertops after autoscaling and the Hotelling T^2 and SPE plots using the remaining 48 countertops as test data are shown in Fig. 8. Using these plots, image number 54A–D, 58A–D, 75A–D, 79A–D, 85A–D, 88A–D, and 90A–D are detected as off-specification countertops. Slab numbers 54, 58, and 75 were already detected as off-specification countertops by the industrial experts. Furthermore, the PCA analysis in Sect. 3.2 can provide additional interpretation about the off-specification countertops. For example, slab number 90 is off-specification because it has more fine scale structure (a positive t_1 score), lower contrast (a negative t_2 score), and clearer quartz edges (a positive t_3 score) compared to good batch countertops (see Fig. 3). With this information, operators can decide the direction of corrective actions on operating conditions in order to achieve the desired aesthetic quality during the batch.

4 Conclusion

Machine vision in a new paradigm is developed for the consistent and quantitative estimation of appearance/aesthetics for products with a stochastic textural appearance. The method is applied to quantify and monitor the appearance of industrially manufactured stone countertops. The method can easily be extended to combine both spectral and textural appearance for colored products [9]. The new paradigm also opens opportunities for many systems engineering tasks such as modeling, monitoring, control, and optimization of visual quality of products or processes [4, 5].

Acknowledgements Authors thank Dupont Canada, and Steve Whitworth and Paul Nomikos for providing the data for this study.

References

1. Davies, E.R.: Machine Vision: Theory, Algorithms, Practicalities, 2nd edn. Academic Press, San Diego, CA (1997)
2. Marshall, A.D., Martin, R.R.: Computer Vision, Models and Inspection. World Scientific Publishing, Singapore (1992)
3. Hyper Dictionary: http://www.hyperdictionary.com/search.aspx?define=computer±vision
4. Liu, J., MacGregor, J.F., Duchesne, C., Bartolacci, G.: Monitoring of flotation processes using multiresolutional multivariate image analysis. Miner. Eng. **18**(1), 65–76 (2005)
5. Liu, J., MacGregor, J.F.: Modeling and optimization of product appearance: application to injection-molded plastic panels. Ind. Eng. Chem. Res. **44**, 4687–4696 (2005)
6. Bharati, M., Liu, J., MacGregor, J.F.: Image texture analysis: methods and comparisons. Chemometrics Intell. Lab. Syst. **72**(1), 57–71 (2004)
7. Honglu, Y., MacGregor, J.F., Haarsma, G., Bourg, W.: Digital imaging for on-line monitoring and control of industrial snack food processes. Ind. Eng. Chem. Res. **42**(13), 3036–3044 (2003)
8. Honglu, Y., MacGregor, J.F.: Monitoring flames in an industrial boiler using multivariate image analysis. AIChE J. **50**(7), 1474–1483 (2004)
9. Liu, J., MacGregor, J.F.: On the extraction of spectral and spatial information for image analysis. Chemometrics Intell. Lab. Syst. (2004)
10. Mallat, S.G.: A theory for multiresolution signal decomposition: The wavelet representation. IEEE Trans. Pattern Anal. Mach. Intell. **11**(7), 674–693 (1989)
11. Rioul, O., Duhamel, P.: Fast algorithms for discrete and continuous wavelet transforms. IEEE Trans. Inform. Theory **38**(2), 569–586 (1992)
12. Daubechies, I.: Ten lectures on wavelets. In: Proceedings of the CBMS-NSF Reg. Conf. Series in Applied Math. no. 61. SIAM, Philadelphia, PA (1992)
13. Vetterli, M., Kovaević, J.: Wavelets and Subband Coding. Prentice Hall, Englewood Cliffs, NJ (1995)
14. Randen, T., Husoy, J.H.: Filtering for texture classification: a comparative study. IEEE Trans. Pattern Anal. Mach. Intell. **21**(4), 291–310 (1999)
15. Tuceryan, M., Jain, A.K.: Texture analysis. In: Chen, C.H., et al., (eds.) Handbook of Pattern Recognition and Computer Vision, 2nd edn., pp. 235–276. World Scientific Publishing, New Jersey (1993)
16. Chang, T., Kuo, C.C.J.: Texture analysis and classification with tree-structured wavelet transform. IEEE Trans. Image Process. **2**(4), 429–441 (1993)
17. Etdmad, K., Chellappa, R.: Separability-based multiscale basis selection and feature extraction for signal and image classification. IEEE Trans. Image Process. **7**(10), 1453–1465 (1998)
18. Laine, A., Fan, J.: Texture classification by wavelet packet signatures. IEEE Trans. Pattern Anal. Mach. Intell. **15**(11), 1186–1191 (1993)
19. Hotelling, H.: Analysis of a complex of statistical variables into principal components. J. Educ. Psychol. **24**, 417–441 (1933)
20. Karhunen, K.: Uber lineare methoden in der Wahrscheilichkeitsrechnung. Ann. Acad. Sci. Fenn., Ser. A1: Math.-Phys. **37**, 3–79 (1947)
21. Loéve, M.: Probability Theory. Van Nostrand, New York (1963)
22. Fisher, R.A.: The use of multiple measurements in taxonomic problems. Ann. Eugen. **7**(Part II), 179–188 (1936)
23. Bell, A.J., Sejnoski, T.J.: An information-maximization approach to blind separation and blind deconvolution. Neural Comput. **7**, 1129–1159 (1995)
24. Friedman, J.H., Tukey, J.W.: A projection pursuit algorithm for exploratory data analysis. IEEE Trans. Comput. **23**(9), 881–890 (1974)
25. Kresta, J.V., MacGregor, J.F., Marlin, T.E.: Multivariate statistical monitoring of process operating performance. Can. J. Chem. Eng. **69**, 35–47 (1991)
26. Kourti, T., MacGregor, J.F.: Multivariate statistical process control methods for monitoring and diagnosing process and product performance. J. Qual. Technol. **28**, 409–428 (1996)
27. Jackson, J.E.: A User's Guide to Principal Components. Wiley-Interscience, New York (1991)

28. Lee, J.-.M, Yoo, C., Lee, I.B.: Statistical process monitoring using independent component analysis. J. Process Control **14**(5), 467–485 (2004)
29. Mojsilović, A., Popović, M.V., Rackkov, D.M.: On the selection of an optimal wavelet basis for texture characterization. IEEE Trans. Image Process. **9**(12), 2043–2050 (2000)
30. Besse, P., de Falguerolles, A.: Application of resampling methods to the choice of dimension in principal component analysis. In: Härdle, W., Simar, L. (eds.) Computer Intensive Methods in Statistics, pp. 167–174. Physica-Verlag, Heidelberg, Germany (1993)
31. Gonzalez, R.C., Woods, R.E.: Digital Image Processing. Addison-Wesley, Reading, MA (1993)